

# Diffusion basis spectrum imaging (DBSI) and manganese-enhanced MRI (MEMRI) detect axonal pathologies with decreased axonal transport in optic nerves of DBA/2J mice

Chia-Wen Chiang<sup>1</sup>, Tsen-Hsuan Lin<sup>2</sup>, Joong Hee Kim<sup>1</sup>, and Sheng-Kwei Song<sup>1,3</sup>

<sup>1</sup>Radiology, Washington University School of Medicine, St. Louis, MO, United States, <sup>2</sup>Physics, Washington University, St. Louis, MO, United States,

<sup>3</sup>The Hope Center for Neurological Disorders, Washington University School of Medicine, St. Louis, MO, United States

## Introduction

Glaucoma is the leading cause of blindness worldwide. Although the pathogenesis of glaucoma is not fully understood, both the retinal ganglion cell and its axons, the optic nerves, are injured in glaucoma. In this study, *in vivo* diffusion basis spectrum imaging (DBSI) and manganese-enhanced MRI (MEMRI) were performed to assess axonal pathologies (inflammation, demyelination and axonal injury) and to determine the degree of axonal transport deficit in 12-month old DBA/2J mice, a rodent model of glaucoma which develops progressive degeneration of visual function mimicking human glaucoma. Our results suggest that DBA/2J mice developed inflammation, axonal injury, demyelination with significant axonal transport disruption in optic nerves compared with the age-matched controls.

## Materials and Methods

**Animal Model:** DBA/2J (male/female = 3/3), and age-matched WT (male/female = 3/2) mice at 12 months old were examined. **DBSI:** A pair of 8-cm diameter volume and 1.7-cm diameter surface active-decoupled coils was used. DBSI was performed on a 4.7-T Agilent small-animal MR scanner utilizing a spin-echo diffusion-weighted sequence with a 25-direction diffusion weighting scheme (25-direction and 25-b-value) was performed. All images were obtained with following acquisition parameters: TR = 1.5 s, TE = 37 ms,  $\Delta$  = 18 ms,  $\delta$  = 6 ms, maximal b-value = 2,200 s/mm<sup>2</sup>, slice thickness = 0.8 mm, FOV (field of view) = 22.5  $\times$  22.5 mm<sup>2</sup>, in-plane resolution = 117  $\times$  117  $\mu$ m<sup>2</sup> (before zero-filled). **MnCl<sub>2</sub> injection:** 3–4 days post-DBSI scans, an intravitreal injection of 50 nmol MnCl<sub>2</sub> (0.25  $\mu$ L of 0.2 M, at 3  $\mu$ L/min) was performed on one eye from both DBA/2J and WT mice with 34-gauge needle<sup>4</sup>. After injection, mice were returned to regular cages for recover from the anesthesia. **MEMRI:** after one hour post-injection, experiments were performed on the same scanner as DBSI using a standard 3D gradient echo sequence with the following parameters: TR = 15 ms, TE = 2.63 ms, flip angle = 20°, FOV = 15  $\times$  15  $\times$  22 mm<sup>3</sup>, matrix size = 128  $\times$  128  $\times$  64 (zero-filled to 256  $\times$  256  $\times$  128), acquisition time = 32.8 minutes, number of signals averaged = 16, and ten successive sets of 3D-T1W images were captured ~1.55 – 5.4 hours post-injection. The active-decoupled coils for MEMRI were the same as DBSI. **B1-inhomogeneity correction:** 3D-T1W image of a 2% agar gel phantom was placed underneath surface coil using the same MEMRI acquisition parameters with 64 averages. The raw 3D-T1W image of mouse brain was divided by the 3D-T1W image of phantom voxel by voxel using ImageJ to correct the 3D-T1W image. **Data analysis:** **DBSI:** 25 diffusion weighted signals and one signal at b = 0 were fitted into a linear combination of one anisotropic diffusion and multiple isotropic diffusion tensor components to estimate  $\lambda_{\parallel}$ ,  $\lambda_{\perp}$  fractions of restricted (putative cellularity) and non-restricted isotropic diffusion (putative vasogenic edema) using in-house DBSI computation package. **Transport rate calculation:** The corrected 3D-T1W image set was adjusted and rotated to an oblique plane covering retina and optic nerves before optic chiasm (Fig. 2A). Line ROIs were drawn on Mn<sup>2+</sup>-loading and contralateral optic nerves for all oblique corrected T1W images (Fig. 2B). Arrival of Mn<sup>2+</sup> was determined by intensity of voxel  $\geq$  thresholds (mean + 2SD of contralateral ROI line). The slope of normalized displacement normalized by entire optic-nerve length was defined as the transport rate in millimeters per hour (Fig. 2C and D). **Histology:** Mice were perfusion fixed immediately after *in vivo* MEMRI measurements for immunohistochemical (IHC) staining of the optic nerve with SMI-31, MBP and DAPI.

## Results

Comparing to control mice, DBA/2J mice exhibited a statistically significant 16% lower DBSI- $\lambda_{\parallel}$  ( $p < 0.005$ ) and 87% higher inflammation (sum of restricted and non-restricted diffusion fraction;  $p < 0.005$ ). Mild demyelination was seen in DBA/2J mouse optic nerves. Axonal transport rate was significantly decreased by 58% from that of control mice.

Representative IHC images suggest axonal injury (decreased SMI-31), demyelination (less MBP positive area), and inflammation (increased number of DAPI positive nuclei) in DBA/2J mouse optic nerves.

## Conclusion

Our results demonstrated that DBSI not only detects axonal pathologies but also reflect inflammation. MEMRI, as has been shown in the literature, is readily applicable for *in vivo* axonal transport assessments in animal models. The current finding suggests that DBSI could potentially play a role in assessing optic nerve pathology in patients to understand the role of axonal degeneration in glaucoma related blindness.

## Reference

[1] Quigley and Broman ; British J of Ophthalmol 2006; 90: 262-267; [2] Wang et al., Brain 2011, 134 :3590-3601 [3] Chiang et al., Proc. Intl. Soc. Magn. Reson. Med. 20 (2012), 3085; [4] Chan et al., Investigativ Ophthalmology & Visual Science 2012; 53 :2777-2785

## Acknowledgements

Supported in part by NIH R01-NS047592, P01-NS059560, NMSS RG 4549A4/1, and DOD W81XWH-12-1-0457

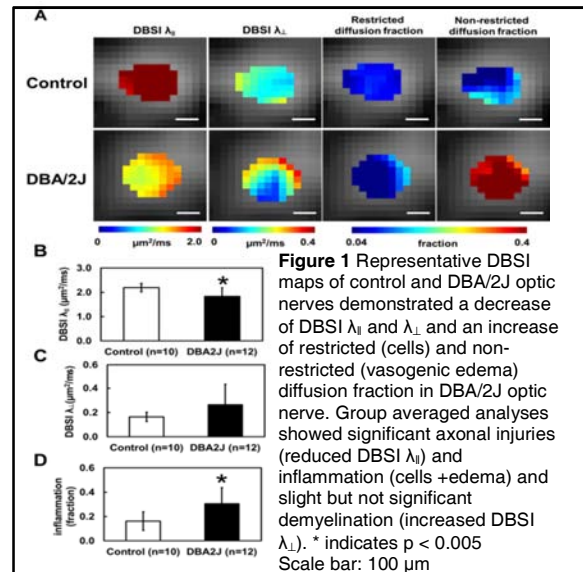


**Figure 1** Representative DBSI maps of control and DBA/2J optic nerves demonstrated a decrease of DBSI  $\lambda_{\parallel}$  and  $\lambda_{\perp}$  and an increase of restricted (cells) and non-restricted (vasogenic edema) diffusion fraction in DBA/2J optic nerve. Group averaged analyses showed significant axonal injuries (reduced DBSI  $\lambda_{\parallel}$ ) and inflammation (cells +edema) and slight but not significant demyelination (increased DBSI  $\lambda_{\perp}$ ). \* indicates  $p < 0.005$   
Scale bar: 100  $\mu$ m

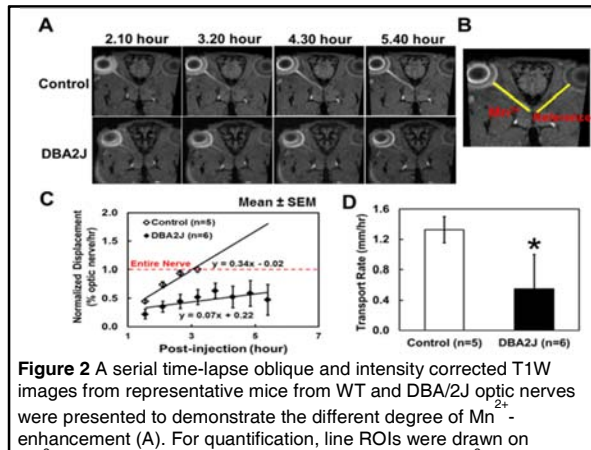


**Figure 2** A serial-lapse oblique and intensity corrected T1W images from representative mice from WT and DBA/2J optic nerves were presented to demonstrate the different degree of Mn<sup>2+</sup> enhancement (A). For quantification, line ROIs were drawn on Mn<sup>2+</sup>-loading and contralateral nerves (B). Arrival of Mn<sup>2+</sup> was determined by threshold and normalized by whole length of the optic nerve. Normalized displacement of WT and DBA/2J mice at each time point showed different axonal transport rates (C). A significant axonal transport disruption was seen in optic nerves from DBA/2J mice. \* indicates  $p < 0.005$

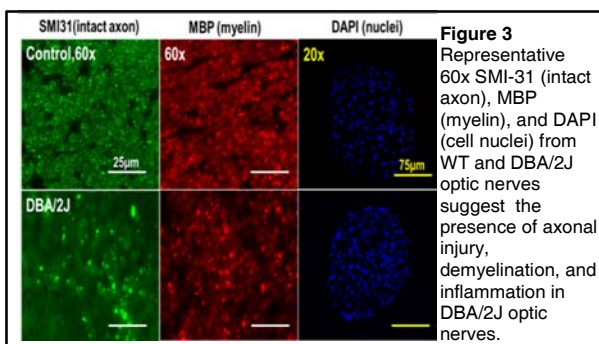


**Figure 3** Representative 60x SMI-31 (intact axon), MBP (myelin), and DAPI (nuclei) from WT and DBA/2J optic nerves suggest the presence of axonal injury, demyelination, and inflammation in DBA/2J optic nerves.